

$[^{11}\text{C}]$ -L-Methionine positron emission tomography in the management of children and young adults with brain tumors

Norbert Galldiks · Lutz W. Kracht · Frank Berthold ·
Hrvoje Miletic · Johannes C. Klein · Karl Herholz ·
Andreas H. Jacobs · Wolf-Dieter Heiss

Received: 4 March 2009 / Accepted: 22 June 2009 / Published online: 4 July 2009
© The Author(s) 2009. This article is published with open access at Springerlink.com

Abstract Only a few *Methyl*- $[^{11}\text{C}]$ -L-methionine (MET) positron emission tomography (PET) studies have focused on children and young adults with brain neoplasm. Due to radiation exposure, long scan acquisition time, and the need for sedation in young children MET-PET studies should be

restricted to this group of patients when a decision for further therapy is not possible from routine diagnostic procedures alone, e.g., structural imaging. We investigated the diagnostic accuracy of MET-PET for the differentiation between tumorous and non-tumorous lesions in this group of patients. Forty eight MET-PET scans from 39 patients aged from 2 to 21 years (mean 15 ± 5.0 years) were analyzed. The MET tumor-uptake relative to a corresponding control region was calculated. A receiver operating characteristic (ROC) was performed to determine the MET-uptake value that best distinguishes tumorous from non-tumorous brain lesions. A differentiation between tumorous ($n = 39$) and non-tumorous brain lesions ($n = 9$) was possible at a threshold of 1.48 of relative MET-uptake with a sensitivity of 83% and a specificity of 92%, respectively. A differentiation between high grade malignant lesions (mean MET-uptake = 2.00 ± 0.46) and low grade tumors (mean MET-uptake = 1.84 ± 0.31) was not possible. There was a significant difference in MET-uptake between the histologically homogeneous subgroups of astrocytoma WHO grade II and anaplastic astrocytoma WHO grade III ($P = 0.02$). MET-PET might be a useful tool to differentiate tumorous from non-tumorous lesions in children and young adults when a decision for further therapy is difficult or impossible from routine structural imaging procedures alone.

Norbert Galldiks and Lutz W. Kracht have contributed equally to this work.

N. Galldiks (✉)
Department of Neurology, University of Cologne, Kerpener Str.
62, 50924 Cologne, Germany
e-mail: Norbert.Galldiks@uk-koeln.de

L. W. Kracht · J. C. Klein · K. Herholz ·
A. H. Jacobs · W.-D. Heiss
Max Planck-Institute for Neurological Research, Cologne,
Germany

F. Berthold
Department of Paediatric Oncology, University of Cologne,
Cologne, Germany

H. Miletic
Department of Neuropathology, University of Cologne, Cologne,
Germany

Present Address:
K. Herholz
Wolfson Molecular Imaging Centre, University of Manchester,
Manchester, UK

Present Address:
A. H. Jacobs
Department of Neurology, Klinikum Fulda, Germany

Present Address:
J. C. Klein
Department of Neurology, University of Frankfurt, Frankfurt,
Germany

Keywords Brain tumor · Children · PET · Methionine · Molecular imaging

Introduction

Methyl- $[^{11}\text{C}]$ -L-methionine (MET) positron emission tomography (PET) is a well established method in the diagnosis and management of adult patients suffering from

brain tumors. Besides less common tumors of the cranial cavity (e.g., embryogenic tumors, glioneural tumors, lymphomas, meningiomas) MET is incorporated into malignant gliomas (e.g., anaplastic astrocytoma, anaplastic oligoastrocytoma, anaplastic oligodendroglioma, glioblastoma multiforme), even in low grade gliomas (e.g., WHO-grade II astrocytoma), and it is employed in the management of these patients [1, 2]. MET is a sensitive tracer in tumor detection. In adults, it differentiates benign from malignant lesions with high sensitivity and specificity with comparatively low background activity in normal brain tissue [1, 2]. MET-uptake correlates to cell proliferation in cell culture [3], Ki-67 expression [4], cell nuclear antigen expression [5] and microvessel density [6], indicating its role as a marker for active tumor proliferation and angiogenesis. In addition it seems to be useful in monitoring chemotherapy in patients with brain tumors [7, 8]. The main advantage of amino acid tracers when compared to [¹⁸F]-2-fluoro-2-deoxy-D-glucose (FDG) is the excellent delineation of tumors extent [9].

Despite this good imaging properties of MET-PET only a few studies have focused on children and young adults with brain neoplasms [10–12]. Pirotte and co-workers provided evidence that MET- and FDG-PET improves the diagnostic yield in stereotactic brain biopsies and surgical management of brain tumors in children [11, 13, 14].

In planning a PET scan for a child, various aspects need consideration. For practical use and implementation of PET in children see Borgwardt et al. [15]. Because molecular imaging can not replace structural imaging modalities like magnetic resonance imaging (MRI) or computed tomography (CT), it is always a supplementary investigation with radioactive exposure and comparatively long scan times. In respect of the effective radiation dose, whole-body distribution of FDG in children differed from adults: a greater proportion of the injected activity accumulated into the brain and less was excreted to urine [16]. The dose of the injected radionuclide has to be adjusted for body weight. In addition, in children sedation or even general anesthesia especially in very young children is necessary to avoid patient movement. PET should be restricted to children with brain tumors where a clear decision for further therapy planning is not possible from structural routine imaging alone.

We investigated the diagnostic accuracy of MET-PET for the differentiation between tumorous and non-tumorous lesions in this selected group of patients.

Patients and methods

Patients

Thirty-nine patients were included in the study. At the time of MET-PET investigation, the mean age of all patients

was 15 ± 5.0 years (range 2–21 years). The patients were referred to the PET-unit of the Max-Planck-Institute for Neurological Research in Cologne, Germany because decision from MRI findings was difficult for further diagnostic procedures or therapy planning. A total of 48 MET-PET scans were performed for all patients. Two or more investigations were performed in 6 patients during follow up. The purpose of the scan and potential risks were explained to the patients or their legal guardians before they gave their informed consent to the investigation.

In order to differentiate between children and young adults, the threshold of age was set at 15 years. In the literature, a clear definition of a young adult was not available; therefore, the threshold of 15 years was set in the middle of the period of life between 10 and 20 years, which is the current definition of adolescence by the World Health Organization (WHO). In our collective, at the time of MET-PET imaging 17 patients were under the age of 15 years.

To evaluate the diagnostic accuracy of MET-PET for the differentiation between tumorous and non-tumorous lesions in this group of patients, routine diagnostic procedures like histological examinations and follow-up structural imaging (MRI or CT scans with contrast enhancing agents) were performed. Follow-up structural imaging was performed to confirm or to exclude a change of the lesion size over the course of the disease. Structural imaging procedures were performed within the clinical routine periodically every 3–12 months, depending on the WHO-grade of the brain tumor. E.g., a low-grade tumor was examined every 12 months, a WHO-grade IV tumor was examined every 3–6 months. Recurrence of a brain tumor was defined according to the Macdonald criteria (gadolinium enhancement or tumor enlargement $\geq 25\%$) [17]. Furthermore, after clinical deterioration or occurrence of new symptoms, structural imaging was performed promptly. After MET-PET imaging, the mean follow-up (imaging procedures like MRI or CT and/or clinically) was 25.5 ± 43.3 months. Additionally, clinical aspects like an asymptomatic course of the disease, therapy response (e.g. anticonvulsive medication, corticosteroids) or a deterioration of symptoms were considered as well.

In all patients in which a tumorous lesion ($n = 31$) was suspected (primary tumor or recurrent/residual tumor), the diagnosis was confirmed histologically during the course of the disease (Tables 1, 2). In patients with a non-tumorous lesion ($n = 8$), the diagnosis was confirmed histologically, clinically, by imaging results (MRI or CT scan), or clinically in combination with follow-up imaging results (Table 1).

In 16 MET-PET scans of 15 patients (5 patients under the age of 15 years) a primary brain tumor was suspected on MRI (Table 3). In these patients MET-PET was

performed to confirm MRI findings and to give additional information about extent and dignity of the lesion.

Presence or absence of a primary tumor at the time of MET-PET imaging ($n = 16$ in 15 patients) was confirmed (i) histologically after the MET-PET examination by surgery or stereotactic biopsy ($n = 8$), (ii) clinically ($n = 4$), (iii) or by follow-up MRI or CT scans ($n = 3$).

In 21 MET-PET scans of 20 patients (11 patients under the age of 15 years) a recurrent or residual tumor was suspected after therapy, but a clear differentiation from posttherapeutic changes was not possible from MRI alone (Table 4).

Presence or absence of a recurrent or residual tumor with previously histologically confirmed diagnosis at the time of MET-PET imaging ($n = 21$ in 20 patients) was confirmed (i) by further histological diagnosis after surgery or stereotactic biopsy ($n = 5$), (ii) clinically ($n = 2$), (iii) by follow-up MRI or CT scans ($n = 5$), (iv) or clinically in combination with follow-up imaging results ($n = 8$).

Additionally, 4 patients were examined initially when a primary brain tumor was suspected on MRI and, afterward, when a recurrent or residual tumor was suspected after therapy (Table 5). In these 4 patients, 11 MET-PET scans were performed (one patient of these 4 patients was under the age of 15 years).

Presence of primary tumor and recurrent or residual tumor, respectively, was confirmed (i) both histologically ($n = 1$), (ii) clinically and histologically ($n = 1$), (iii) or clinically in combination with imaging results and histologically ($n = 2$).

Most tumors were located in critical areas like basal ganglia, midbrain, and brainstem or next to motor areas in the pericentral region or speech relevant areas in the left temporal lobe.

Methods

Altogether, 48 MET-PET studies of the 39 patients were performed either on an ECAT EXACT HR or ECAT EXACT scanner (Siemens-CTI, Knoxville, TN) [18, 19]. In one child a mild sedation and in four children a general anesthesia was necessary to avoid patient movement. In these cases, the children were under the age of 12 years. 11 MBq/kg bodyweight MET (maximum 740 MBq) were injected intravenously. MET was synthesized according to the method of Berger et al. [20]. Tracer accumulation was recorded over 60 min directly after tracer injection or over 40 min beginning 20 min after tracer injection. The entire brain was scanned in 47 transaxial slices. Summed activity from 20 to 60 min after tracer injection was used for image reconstruction. Scans were corrected for attenuation and scatter. Spatial resolution was 6 mm or better in all dimensions.

As described previously, a circular region of interest (ROI) of 7 mm diameter was placed in the area of maximum MET-uptake [21]. Mean uptake of this ROI was determined relative to a control region in the unaffected hemisphere which was obtained by mirroring the ROI along the medial sagittal plane. In midline or brainstem lesions the reference ROI was placed in the fronto-lateral cortex of the unaffected hemisphere.

To determine the relative MET-uptake value that best distinguishes tumorous from non-tumorous brain lesions, a receiver operating characteristic (ROC) analysis was performed by varying the threshold of MET-uptake over the whole range of values and calculating sensitivity and specificity for each value.

For statistical analyses, SPSS version 10.0.7 (SPSS Inc., Chicago, Illinois) was used. Graphs were plotted with SigmaPlot, version 7.0 (SPSS Inc., Chicago, Illinois).

Results

At a threshold of 1.48, relative MET-uptake differentiation between tumorous ($n = 39$) and non-tumorous brain lesions ($n = 9$) was possible with a sensitivity of 83% and specificity of 92% (area under the curve = 0.94, 95%-confidence interval = 0.87–1.00; Fig. 1). At this threshold, 8 of 9 non-tumorous lesions were classified correctly by using MET-PET imaging. The false-positive case was one patient with a newly developed contrast enhancing lesion in the pons 14 years after treatment of a medulloblastoma with a MET-uptake of 1.53. This lesion disappeared slowly without treatment in follow-up MRI examinations 1 and 4 months after the PET investigation. At a threshold greater than 1.53, the specificity was 100% without false positive findings.

Thirty-four of 39 confirmed tumors were correctly classified positive. False negative findings included two pilocytic astrocytoma WHO grade I and two diffuse astrocytoma WHO grade II. In one child with a suspected medulloblastoma, several small areas with a slight MET-uptake of 1.22 were observed. However, this uptake had to be classified as false negative, because a manifest tumor progression could be diagnosed 5 months later.

At a threshold of 1.48, relative MET-uptake differentiation between tumorous and non-tumorous brain lesions was possible in the group of patients under the age of 15 years ($n = 17$) with a sensitivity of 91% and a specificity of 100%.

The mean MET-uptake in 17 high grade tumors [astrocytoma, oligoastrocytoma WHO grade III; ependymoblastoma; glioblastoma, medulloblastoma, atypical teratoid rhabdoid tumor (ATRT) WHO grade IV] was 2.00 ± 0.46 . In comparison to 22 low grade tumors [pilocytic astrocytoma,

Table 1 Individual patient data

Pat. no.	Age [years]	Gender (F = female, M = male)	Diagnosis	WHO grade	Localization	Newly diagnosed (ND)/recurrence (REC)	Sx ^a	Rx ^b	Cx ^c
1	17	F	Pilocytic astrocytoma	I	Right fronto- parietal	ND	No	No	No
2	13	M	Pilocytic astrocytoma	I	3rd ventricle	REC	Yes	No	No
3	16	F	Pilocytic astrocytoma	I	Left thalamus	REC	No	Yes	No
4	11	F	Pilocytic astrocytoma	I	Right basal ganglia	ND	No	No	No
5	19	M	Pilocytic astrocytoma	I	Sellar region	REC	No	Yes	No
6	12	M	Pilocytic astrocytoma	I	Right basal ganglia	REC	No	Yes	No
7	14	F	DNT	I	Left temporal	ND	No	No	No
8	17	M	DIG	I	Left temporal	ND	No	No	No
9	10	M	Astrocytoma	II	Right parietal	ND	No	No	No
10	8	M	Astrocytoma	II	Left temporal	ND	No	No	No
11	21	F	Astrocytoma	II	Left temporal	ND/REC ^d	No	No	No
12	21	F	Astrocytoma	II	Left precentral	ND/REC ^d	No	Yes	No
13	20	M	Astrocytoma	II	Left frontal	REC	Yes	Yes	Yes
14	4	F	Astrocytoma	II	Quadrigeminal plate	ND	No	No	No
15	10	M	Pleomorphic xanthoastrocytoma	II	Left temporal	ND/REC ^d	Yes	No	No
16	13	M	Ependymoma	II	Left cerebellum	REC	No	Yes	No
17	20	F	Astrocytoma	III	Right thalamus	REC	No	Yes	No
18	21	F	Astrocytoma	III	Right basal ganglia	REC	No	Yes	No
19	14	M	Astrocytoma	III	Left pericentral	REC	Yes	Yes	No
20	14	F	Astrocytoma	III	Right frontal	REC	Yes	Yes	No
21	19	F	Oligoastrocytoma	III	Left temporo-parietal	ND/REC ^d	Yes	Yes	Yes
22	21	F	Oligoastrocytoma	III	Right internal capsula	REC	Yes	Yes	No
23	18	M	Glioblastoma	IV	Left temporal	REC	Yes	Yes	Yes
24	12	F	Glioblastoma	IV	Right thalamus	REC	Yes	Yes	Yes
25	20	F	Medulloblastoma	IV	Left cerebellum	REC	Yes	Yes	Yes
26	10	F	Medulloblastoma	IV	Right frontal	REC	Yes	Yes	No
27	21	M	Medulloblastoma	IV	Pons	REC	Yes	Yes	Yes
28	8	F	Medulloblastoma	IV	Right cerebellum	REC	Yes	No	Yes
29	11	F	Ependymoblastoma	IV	Right fronto-temporal	REC	Yes	Yes	No
30	2	F	ATRT	IV	Brainstem	REC	Yes	No	Yes
31	9	M	ATRT	IV	Right temporo-occipital	REC	Yes	No	No
32	19	M	Cortical malformation	/	Right temporal	ND	No	No	No
33	19	F	Cortical malformation	/	Left temporal	ND	No	No	No
34	21	M	Epilepsy	/	Right fronto-parietal	ND	No	No	No
35	18	F	Pineal cyst	/	Pineal gland	ND	No	No	No
36	19	F	ADEM	/	Right occipital	ND	No	No	No
37	18	F	Multiple sclerosis	/	Left parieto-occipital	ND	No	No	No
38	20	F	Multiple sclerosis	/	Left occipital	ND	No	No	No
39	18	M	Stroke PCA	/	Left occipital	ND	No	No	No

Individual data of 39 children and young adults with suspected newly diagnosed or recurrent brain tumor who underwent MET-PET

DIG Desmoplastic infantile ganglioglioma, *DNT* dysembryoplastic neuroepithelial tumor, *ATRT* atypical teratoid rhabdoid tumor, *ADEM* acute demyelinating encephalomyelitis, *PCA* posterior cerebral artery

^a Surgery before MET-PET

^b Radiation therapy before MET-PET

^c Chemotherapy before MET-PET

^d Patients were investigated at the time of first diagnosis and at the time of suspected recurrence

Table 2 Number of patients with tumors of different histological types and non-tumorous lesions

Histological diagnosis and WHO grade	Total	Under age of 15	15–21 years
Histological diagnoses			
Pilocytic astrocytoma I	6	3	3
Astrocytoma II	6	3	3
Pleomorphic xanthoastrocytoma II	1	1	0
Astrocytoma III	4	2	2
Oligoastrocytoma III	2	0	2
Glioblastoma IV	2	1	1
Medulloblastoma IV	4	2	2
Atypical teratoid rhabdoid tumor IV	2	2	0
Ependymoma II	1	1	0
Ependymoblastoma IV	1	1	0
DNT I	1	1	0
Desmoplastic infantile ganglioglioma I	1	0	1
Non-tumor lesions	8	0	8
Total	39	17	22

Table 3 Patients with a suspected primary brain tumor on MRI

#	Pat. no.	Age [years]	Gender (F = female, M = male)	Diagnosis	WHO grade	Localization	Number of MET-PET scans [n]	Diagnosis confirmed by
1	1	17	F	Pilocytic astrocytoma	I	Right fronto-parietal	1	1
2	4	11	F	Pilocytic astrocytoma	I	Right basal ganglia	1	1
3	7	14	F	DNT	I	Left temporal	1	1
4	8	17	M	DIG	I	Left temporal	1	1
5	9	10	M	Astrocytoma	II	Right parietal	1	1
6	10	8	M	Astrocytoma	II	Left temporal	1	1
7	14	4	F	Astrocytoma	II	Quadrigeminal plate	1	1
8	32	19	M	Cortical malformation	/	Right temporal	1	2
9	33	19	F	Cortical malformation	/	Left temporal	1	2
10	34	21	M	Epilepsy	/	Right fronto-parietal	1	3
11	35	18	F	Pineal cyst	/	Pineal gland	1	2
12	36	19	F	ADEM	/	Right occipital	2	1
13	37	18	F	Multiple sclerosis	/	Left parieto-occipital	1	3
14	38	20	F	Multiple sclerosis	/	Left occipital	1	2
15	39	18	M	Stroke PCA	/	Left occipital	1	3

In these patients PET was performed to confirm MRI findings and to give additional information about extent and dignity of the lesion. Diagnosis was confirmed (1) histologically after the MET-PET examination by surgery or stereotactic biopsy, (2) clinically, (3) or by follow-up MRI or CT scans

dysembryoplastic neuroepithelial tumor (DNT), desmoplastic infantile ganglioglioma (DIG) WHO grade I; diffuse astrocytoma, pleomorphic xanthoastrocytoma WHO grade II], the mean MET-uptake was lower (1.84 ± 0.31). However, a differentiation between low grade and high grade tumors was not possible (Student’s *t*-test; $P = 0.36$). MET-uptake in the different histological tumor types and WHO grades is summarized in Table 6.

The MET-uptake differed significantly (Student’s *t*-test; $P = 0.02$) when focused on the histologically more homogeneous subgroup of diffuse astrocytoma WHO grade II (1.69 ± 0.50) and anaplastic astrocytoma WHO grade III (2.61 ± 0.73).

The MET-uptake in WHO grade I tumors, especially in pilocytic astrocytomas (2.11 ± 0.88) was higher when compared to WHO grade II astrocytomas (1.69 ± 0.50),

Table 4 Patients with suspected recurrent tumor after therapy in which a clear differentiation from posttherapeutic changes was not possible from MRI alone

#	Pat. no.	Age [years]	Gender (F = female M = male)	Diagnosis	WHO grade	Localization	Number of MET-PET scans [n]	Diagnosis confirmed by
1	2	13	M	Pilocytic astrocytoma	I	3rd ventricle	1	3
2	3	16	F	Pilocytic astrocytoma	I	Left thalamus	1	3
3	5	19	M	Pilocytic astrocytoma	I	Sellar region	1	1
4	6	12	M	Pilocytic astrocytoma	I	Right basal ganglia	1	3
5	13	20	M	Astrocytoma	II	Left frontal		1
6	16	13	M	Ependymoma	II	Left cerebellum	1	1
7	17	20	F	Astrocytoma	III	Right thalamus	2	4
8	18	21	F	Astrocytoma	III	Right basal ganglia	1	4
9	19	14	M	Astrocytoma	III	Left pericentral	1	1
10	20	14	F	Astrocytoma	III	Right frontal	1	3
11	22	21	F	Oligoastrocytoma	III	Right internal capsula	1	4
12	23	18	M	Glioblastoma	IV	Left temporal	1	4
13	24	12	F	Glioblastoma	IV	Right thalamus	1	4
14	25	20	F	Medulloblastoma	IV	Left cerebellum	1	4
15	26	10	F	Medulloblastoma	IV	Right frontal	1	4
16	27	21	M	Medulloblastoma	IV	Pons	1	1
17	28	8	F	Medulloblastoma	IV	Right cerebellum	1	2
18	29	11	F	Ependymoblastoma	IV	Right fronto-temporal	1	3
19	30	2	F	ATRT	IV	Brainstem	1	2
20	31	9	M	ATRT	IV	Right temporo-occipital	1	4

Diagnosis was confirmed (1) histologically after the MET-PET examination by surgery or stereotactic biopsy, (2) clinically, (3) by follow-up MRI or CT scans, (4) or clinically in combination with follow-up imaging results

Table 5 Patients with brain tumor which were examined initially when a primary brain tumor was suspected on MRI and, afterward, when a recurrent or residual tumor was suspected after therapy

#	Pat. no.	Age [years]	Gender (F = female M = male)	Diagnosis	WHO grade	Localization	Number of MET-PET scans [n]	Diagnosis confirmed by
1	11	21	F	Astrocytoma	II	Left temporal	2	4,1
2	12	21	F	Astrocytoma	II	Left precentral	2	2,1
3	15	10	M	Pleomorphic xanthoastrocytoma	II	Left temporal	5	1,1
4	21	19	F	Oligoastrocytoma	III	Left temporo-parietal	2	4,1

Diagnosis was confirmed (1) histologically after the MET-PET examination by surgery or stereotactic biopsy, (2) clinically, (3) by follow-up MRI or CT scans, (4) or clinically in combination with follow-up imaging results

but the difference did not reach statistical significance (Student's *t*-test; $P = 0.28$).

Discussion

Our findings suggest that MET-PET has diagnostic relevance in a selected patient population including children and young adults and is able to distinguish brain tumors and non-tumorous brain lesions with a high sensitivity (83%) and specificity (92%). Therefore, MET-PET may be

helpful especially in this group of patients when results of structural routine diagnostic procedures are not sufficient enough to obtain a treatment decision and its planning.

Due to the reduced MET-uptake in healthy brain tissue and, therefore, a increased contrast between normal brain tissue and a tumorous lesion, MET-PET is superior to FDG-PET in tumor detection and assessment of tumor dimensions [9, 22, 23]. Utriainen and co-workers described that 22 of 23 childhood brain tumors exhibited higher MET accumulation in the tumor than in the adjacent brain tissue [12]. This observation supports our findings and may

ROC analysis of relative [¹¹C-MET]-uptake to differentiate tumor from non-tumorous lesions

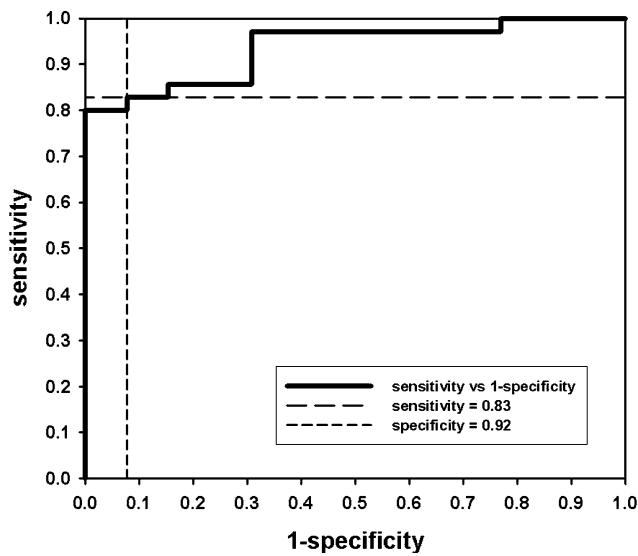


Fig. 1 ROC analysis of relative [¹¹C-MET]-uptake to differentiate tumor from non-tumorous lesions

indicate that MET-PET is not only highly sensitive but also very specific.

However, four low grade tumors (two patients with pilocytic astrocytoma and two patients with astrocytoma WHO grade II) were classified false negative. Low MET-uptake in a proportion of WHO grade II astrocytomas is a known feature of this histological entity in adult patients [21]. In contrast, in our study pilocytic astrocytoma WHO grade I demonstrated relatively high MET-uptake

(2.11 ± 0.88) when compared to astrocytoma WHO grade II (1.69 ± 0.50). This has also been observed in a previous study [21]. Histopathological features of pilocytic astrocytoma include mitosis, microvascular proliferation and infiltration, but are not signs of malignancy in this tumor entity. In adult patients with gliomas, both mitotic activity and increased vascularization correlate with high MET-uptake, which may explain the high MET-uptake in pilocytic astrocytomas [5, 6]. In the two patients with false negative findings, low MET-uptake might be influenced by a decreased degree of microvascular proliferation in the pilocytic astrocytoma.

Additionally, MET-uptake in one patient with suspected recurrent medulloblastoma was false negative in several small areas (uptake ratio of 1.22) and tumor progression occurred 5 months later. However, the uptake pattern of small lesions may be underestimated due to partial volume effects. Modern positron cameras like the ECAT EXACT HR have a transaxial resolution of 3.6 mm full width at half maximum, and, therefore small tumors might be hidden by normal brain uptake. Moderate MET-uptake was also observed in embryonal tumors but all patients with medulloblastoma suffered from recurrent tumor at the time of examination. They had previously undergone chemotherapy and/or radiation therapy or they currently received chemotherapy which might have influenced the tracer uptake [7].

In contrast to findings in adult patients, MET-uptake of low grade tumors did not differ significantly from high grade tumorous lesions [2, 21]. This observation is consistent with the findings of Utriainen and colleagues [12] who found no association between MET-uptake and malignancy

Table 6 Maximum MET-uptake relative to corresponding control region within tumors of different histological types and non tumorous lesions

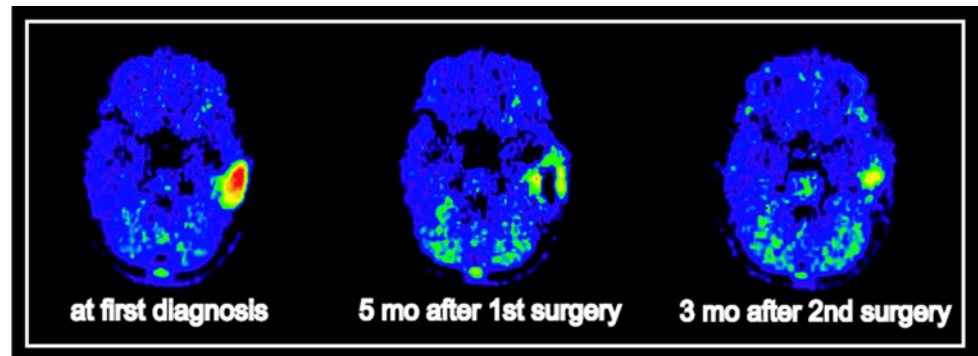
Histological diagnosis and WHO grade	<i>n</i>	<i>n</i> ^a	Relative MET-uptake (mean ± SD ^b)
Relative MET uptake in different tumors			
Pilocytic astrocytoma I	6	6	2.11 ± 0.88
Astrocytoma II	6	8	1.69 ± 0.50
Pleomorphic xanthoastrocytoma II	1	5	2.23 ± 0.48
Astrocytoma III	4	5	2.61 ± 0.73
Oligoastrocytoma III	2	3	2.61 ± 0.24
Glioblastoma IV	2	2	1.70 ± 0.55
Medulloblastoma IV	4	4	1.78 ± 0.55
Atypical teratoid rhabdoid tumor IV	2	2	1.36 ± 0.71
Ependymoma II	1	1	0.97
Ependymoblastoma IV	1	1	1.95
DNT I	1	1	2.04
Desmoplastic infantile ganglioglioma I	1	1	2.01
Non tumor lesions	8	9	1.04 ± 0.22
Total	39	48	

A total of 48 PET investigations were performed in 39 patients

^a Number of MET-PET investigations

^b Standard deviation

Fig. 2 Course of disease in a 10-year-old boy with a pleomorphic xanthoastrocytoma WHO grade II. The tumor is localized in the left temporal lobe (*left image*). In follow-up scans, the tumor recurs early 5 months after initial surgery and 3 months after surgery of recurrent tumor, respectively



grade in childhood tumors. The failure to discriminate low grade from high grade tumors in the whole group probably is due to the confounding effect of high uptake in the pilocytic astrocytomas, which are more frequent in children than in adults. Even in adult patients, non-invasive grading is difficult when the histological subtype of the tumor is unknown because tumors of different histological types and grades show an overlapping pattern in MET-uptake [21]. E.g., oligodendrogliomas WHO grade II might exhibit a MET-uptake comparable to those of anaplastic astrocytoma WHO grade III [6, 21]. If the histological subtype is known, non-invasive grading may be possible in children and young adults, as indicated by the significant difference of MET-uptake between astrocytoma WHO grade II (1.69 ± 0.50) and anaplastic astrocytoma WHO grade III (2.61 ± 0.73). These data suggest that noninvasive diagnosis of malignant progression in gliomas, which is of crucial prognostic and therapeutic interest, may be possible with MET-PET. However, intraindividual changes of MET-uptake in the course of malignant tumor progression in this group of patients have not been investigated systematically so far.

An important differential diagnosis of brain tumors with a slightly increased uptake pattern are inflammatory lesions. In our study a patient with ADEM showed a MET-uptake of 1.45 which is only slightly lower than the threshold of 1.48. This observation might be caused by a disruption of the blood brain barrier due to the inflammation. A small number of acute inflammatory lesions with mild MET-uptake have been observed in previous studies [21, 24, 25].

Sequential MET-PET monitoring of the course of the disease may be helpful in single cases. Figure 2 shows the course of disease in a 10-year-old boy with a pleomorphic xanthoastrocytoma WHO grade II. He was investigated three times using MET-PET within 3 years. The tumor was localized in the left temporal lobe and the patient suffered from mild verbal amnesia at the time of first diagnosis (*left image*). In the histopathological work-up, the tumor yielded areas of increased Ki67-MIB1 proliferation index up to 10. Therefore, close monitoring was recommended. In follow-up scans, the tumor recurred early 5 months after

initial surgery and 3 months after surgery of recurrent tumor, respectively (Fig. 2). This demonstrates that even repeated PET studies may be feasible in a single child revealing important insight into the disease state.

In conclusion, MET-PET in children and young adults is feasible and should be performed after critical consideration of the indication for a MET-PET examination in this group of patients when additional information is needed for the differentiation from non-tumorous lesions before an invasive procedure is initiated.

Acknowledgment We thank Mrs. U. Juchellek, E. Bannemer, R. Rusniak, C. Selbach and A. Derici for their gentle and compassionate care of the little patients and their parents.

Open Access This article is distributed under the terms of the Creative Commons Attribution Noncommercial License which permits any noncommercial use, distribution, and reproduction in any medium, provided the original author(s) and source are credited.

References

- Jacobs AH, Dittmar C, Winkeler A, Garlip G, Heiss WD (2002) Molecular imaging of gliomas. *Mol Imaging* 1(4):309–335
- Jager PL, Vaalburg W, Pruijm J, de Vries EG, Langen KJ, Piers DA (2001) Radiolabeled amino acids: basic aspects and clinical applications in oncology. *J Nucl Med* 42(3):432–445
- Langen KJ, Muhlensiepen H, Holschbach M, Hautzel H, Jansen P, Coenen HH (2000) Transport mechanisms of 3-[123I]iodo-alpha-methyl-L-tyrosine in a human glioma cell line: comparison with [3H]methyl-L-methionine. *J Nucl Med* 41(7):1250–1255
- Chung JK, Kim YK, Kim SK et al (2002) Usefulness of 11C-methionine PET in the evaluation of brain lesions that are hypoor isometabolic on 18F-FDG PET. *Eur J Nucl Med Mol Imaging* 29(2):176–182
- Sato N, Suzuki M, Kuwata N et al (1999) Evaluation of the malignancy of glioma using 11C-methionine positron emission tomography and proliferating cell nuclear antigen staining. *Neurosurg Rev* 22(4):210–214
- Kracht LW, Friese M, Herholz K et al (2003) Methyl-[11C]-L-methionine uptake as measured by positron emission tomography correlates to microvessel density in patients with glioma. *Eur J Nucl Med Mol Imaging* 30(6):868–873
- Herholz K, Kracht LW, Heiss WD (2003) Monitoring the effect of chemotherapy in a mixed glioma by C-11-methionine PET. *J Neuroimaging* 13(3):269–271

8. Galldiks N, Kracht LW, Burghaus L et al (2006) Use of (11)C-methionine PET to monitor the effects of temozolomide chemotherapy in malignant gliomas. *Eur J Nucl Med Mol Imaging* 33(5):516–524
9. Kracht LW, Miletic H, Busch S et al (2004) Delineation of brain tumor extent with [11C]L-methionine positron emission tomography: local comparison with stereotactic histopathology. *Clin Cancer Res* 10(21):7163–7170
10. O'Tuama LA, Phillips PC, Strauss LC et al (1990) Two-phase [11C]L-methionine PET in childhood brain tumors. *Pediatr Neurol* 6(3):163–170
11. Pirotte B, Goldman S, Salzberg S et al (2003) Combined positron emission tomography and magnetic resonance imaging for the planning of stereotactic brain biopsies in children: experience in 9 cases. *Pediatr Neurosurg* 38(3):146–155
12. Utriainen M, Metsahonkala L, Salmi TT et al (2002) Metabolic characterization of childhood brain tumors: comparison of 18F-fluorodeoxyglucose and 11C-methionine positron emission tomography. *Cancer* 95(6):1376–1386
13. Pirotte B, Acerbi F, Lubansu A, Goldman S, Brotchi J, Levivier M (2007) PET imaging in the surgical management of pediatric brain tumors. *Childs Nerv Syst* 23(7):739–751
14. Pirotte B, Goldman S, Dewitte O et al (2006) Integrated positron emission tomography and magnetic resonance imaging-guided resection of brain tumors: a report of 103 consecutive procedures. *J Neurosurg* 104(2):238–253
15. Borgwardt L, Larsen HJ, Pedersen K, Hojgaard L (2003) Practical use and implementation of PET in children in a hospital PET centre. *Eur J Nucl Med Mol Imaging* 30(10):1389–1397
16. Ruotsalainen U, Suhonen-Polvi H, Eronen E et al (1996) Estimated radiation dose to the newborn in FDG-PET studies. *J Nucl Med* 37(2):387–393
17. Macdonald DR, Cascino TL, Schold SC Jr, Cairncross JG (1990) Response criteria for phase II studies of supratentorial malignant glioma. *J Clin Oncol* 8(7):1277–1280
18. Wienhard K, Eriksson L, Grootenck S, Casey M, Pietrzyk U, Heiss WD (1992) Performance evaluation of the positron scanner ECAT EXACT. *J Comput Assist Tomogr* 16(5):804–813
19. Wienhard K, Dahlbom M, Eriksson L et al (1994) The ECAT EXACT HR: performance of a new high resolution positron scanner. *J Comput Assist Tomogr* 18(1):110–118
20. Berger G, Maziere M, Knipper R, Prenant C, Comar D (1979) Automated synthesis of 11C-labelled radiopharmaceuticals: imipramine, chlorpromazine, nicotine and methionine. *Int J Appl Radiat Isot* 30(7):393–399
21. Herholz K, Holzer T, Bauer B et al (1998) 11C-methionine PET for differential diagnosis of low-grade gliomas. *Neurology* 50(5):1316–1322
22. Bergstrom M, Collins VP, Ehrin E et al (1983) Discrepancies in brain tumor extent as shown by computed tomography and positron emission tomography using [68 Ga]EDTA, [11C]glucose, and [11C]methionine. *J Comput Assist Tomogr* 7(6):1062–1066
23. Mosskin M, von Holst H, Bergstrom M et al (1987) Positron emission tomography with 11C-methionine and computed tomography of intracranial tumours compared with histopathologic examination of multiple biopsies. *Acta Radiol* 28(6):673–681
24. Dethy S, Manto M, Kentos A et al (1995) PET findings in a brain abscess associated with a silent atrial septal defect. *Clin Neurol Neurosurg* 97(4):349–353
25. Galldiks N, Burghaus L, Vollmar S et al (2004) Novel neuroimaging findings in a patient with cerebral Whipple's disease: a magnetic resonance imaging and positron emission tomography study. *J Neuroimaging* 14(4):372–376